Effect of Zinc Chloride in Ash in Oxidation Kinetics of Ni-Based and Fe-Based Alloys

E. Schaal, Nicolas David, Pierre-Jean Panteix, C. Rapin, M. Vilasi, S. Mathieu, J. Brossard, F. Maad

Effect of zinc chloride in ash in oxidation kinetics of Ni-based and Fe-based alloy

E. SCHAAL[a] • N. DAVID[a] • P.J. PANTEIX[a] • C. RAPIN[a] • M. VILASI[a] . S. MATHIEU[b] • J.M. BROSSARD[c] • F. MAAD[c]

[a]*Institut Jean Lamour - UMR7198, CNRS - Université de Lorraine, Boulevard des Aiguillettes, BP70239-54506 Vandoeuvre-lès-Nancy Cedex, France*

[b]*Université de Lorraine, Service Commun de Microscopies Electroniques et de Microanalyses X, BP70239-54506 Vandoeuvre-lès-Nancy Cedex, Franc*

[c]*Veolia Recherche et Innovation – Zone portuaire de Limay, 291 Avenue Dreyfous Ducas, 78520 Limay, France*

emmanuel.schaal@univ-lorraine.fr; nicolas.david@univ-lorraine.fr; pierre-jean.panteix@univ-lorraine.fr; christophe.rapin@univ-lorraine.fr; sandrine.mathieu@univ-lorraine.fr; Jean-Michel.BROSSARD@veolia.com; fares.maad@veolia.com.

Abstract

Corrosion by molten phases leads to severe corrosion on heat exchangers in Waste-to-Energy plants. In addition, presence of heavy metal chlorides in ash deposit increases degradation at low temperature due to the formation of highly corrosive molten phases. In this study, two heat exchanger materials, a low alloy steel (16Mo3) and a nickel based alloy (Inconel 625) were exposed in air to three different synthetic ashes, with various chloride contents, including $ZnCl_2$ at isotherm temperatures of 450 °C and 650 °C in a muffle furnace. After the test, thickness and mass losses were evaluated on two separate samples, and metallographic cross sections of the specimens were characterized with a SEM/EDX analyzer. Both measurement results were in good agreement and have shown that the corrosion observed on both materials was higher in presence of zinc chloride in ash at 450 °C than in ashes without heavy metal chloride at 650 °C.

Keywords High temperature corrosion • Zinc chloride • Ashes • Inconel 625 • 16Mo3

Introduction

In Waste-to-Energy (WtE) plants, the composition of ash deposits has a big influence on corrosion rate of superheater's tube [1] which is a major issue in those facilities. WtE's deposits mainly contain calcium sulfates, oxides, alkali chlorides and sulfates and heavy metal chlorides such as $PbCl_2$ and $ZnCl_2$ [2,3,4,5,6,7,8,9]. Those heavy metal chlorides cause accelerated corrosion in WtE environment [9,10] due to the formation of salt mixtures with low temperature melting points. The influence of alkali chlorides content in ash mixtures representative of WtE deposit on the corrosion behavior of 16Mo3 steel and Inconel 625 alloy was studied at temperatures between 450 °C and 650 °C [11]. Two different ashes, one with 10 wt% and one with 40 wt% of chlorides were used for this previous study which allowed to establish that:

- The appearance of molten phases in ashes was correlated with a change of corrosion mechanisms and kinetics,
- Nickel based superalloy (Inconel 625) exhibited very low attack at low temperature (below each ash solidus temperature (T_{sol})) in both ashes contrary to ferritic steel (16Mo3) which was corroded even at 450 °C,
- At 450 °C, corrosion under deposit (active oxidation) was the mechanism responsible of the attack.
- Corrosion rate also increased with the chloride content of ashes. Corrosion increased for both alloys with temperature, and accelerated above T_{sol} of the ash, due to the appearance of molten phases.
- Both evaluation methods, thickness loss and mass loss, were in good agreement and showed that increasing chloride content in ash leaded to higher amount of molten phases, and so, to higher corrosion, especially for low alloy steel (16Mo3).

The present work is focused on the influence of 10 wt% zinc chloride in synthetic ashes on corrosion kinetics in air atmosphere. Results have been compared with those obtained in ashes without heavy metal chlorides [11]. Few studies have been made with heavy metal chlorides in representative ashes,

and their precise effect remains not fully understood yet. They are generally focused on testing deposits composed with one or two species [12,13,14,15,16,17,18,19,20]. First, three synthetic ashes with the same components as those typically found in WtE superheaters tubes and without oxide have been prepared with different heavy metal chlorides content. Those three compositions were synthetized in order to choose one of them based on their corrosivity. The low steel alloy (16Mo3) and the Ni-based superalloy (Inconel 625), were exposed to those ashes at 650 °C during 100 h in order to evaluate the most corrosive ash mixture. Tests in air lab, in crucibles have been performed in the same way as previously [11] in order to compare results and so, to evaluate the influence of heavy metal content in ash on corrosion kinetics. Thickness and mass losses of alloys were the criterions evaluated during this study, which are more relevant than mass gain or oxide layer thickness in order to establish lifetime prediction. Indeed, the residual thickness is the critical criteria for the lifetime of superheater's tubes in WtE plants.

Experimental Procedures

Materials

In this work, the influence of heavy metal chlorides in deposits on corrosion resistance of two alloys has been tested: one ferritic steel (16Mo3, Masteel) and one nickel-based superalloy (Inconel 625, Goodfellow). Table 1 presents the elemental compositions (wt%) given by Masteel and Goodfellow. Metallographic preparation, measurements of thickness and mass of samples were described in earlier study [11].

Physical chemistry of synthetic ashes

Three different synthetic ashes containing 10 wt% of heavy metal chloride were prepared for preliminary tests: one with zinc chloride (# $ZnCl_2$), one with lead chloride (# $PbCl_2$) and one with both heavy metals in equally weighted proportions (# $ZnCl_2$/$PbCl_2$). Their compositions are given in Table 2. Those ashes were prepared with NaCl (99%, SDS), KCl (99.5%, Roth), $ZnCl_2$ (98%, Sigma

Aldrich), $PbCl_2$ (98%, Sigma Aldrich), Na_2SO_4 (98%, VWR), K_2SO_4 (99%, Acros Organics) and $CaSO_4$ (97%, Sigma Aldrich) salts. The same preparation (grounding and mixing) has been performed on ashes with zinc and lead chlorides than the ones made free of heavy metal chlorides. This procedure is described in [11]. Then, results of corrosion obtained after exposure in # $ZnCl_2$ ash were compared to those obtained previously [11] in one chloride rich ash (# 40% Cl) and one chloride poor ash (# 10% Cl). Thermomechanical analyses (TMA, Setaram TMA92 16-18) have also been performed on # $ZnCl_2$ ash as for # 10% Cl and # 40% Cl ashes in order to determine their solidus temperatures (T_{sol}). Differential Thermal Analysis (DTA, Setaram TGA92 16-18) measurements were also performed on # $ZnCl_2$ salts mixtures. In addition, salt mixtures without $CaSO_4$ but keeping proportions between chlorides and sulfates were also prepared and analysed (Table 3). These three ashes have been prepared as comparative basis for ash phase behavior understanding . Indeed, $CaSO_4$ cannot be considered as its interactions with the other salts are not defined in the FactSage Thermodynamic database (FTsalt database [21]).

Corrosion tests

The procedure of corrosion tests was exactly the same as the one defined and described in [11]. Samples were immersed into an alumina crucible with ashes as described in Fig. 1, following the ISO/DIS 17248 standard [22].In preliminary tests, 16Mo3 and Inconel 625 were exposed to the three heavy metal chlorides ashes at 650 °C in ambient air in order to evaluate the corrosivity of those mixtures and choose one ash for the rest of the study. Then, the corrosion tests were performed in ambient air at 2 isothermal temperatures (450 °C and 650 °C). The test temperatures have been chosen to evaluate the influence of heavy metal chlorides in ash at low temperature on corrosion and to compare them with ashes without them at higher temperature. Exposure times were 100, 500 and 1000 h.

Post corrosion tests analyses

After the exposure in ash, the specimens used to measure thickness loss were cut off in the middle and the metallographic cross-sections were characterized with SEM/EDX analyzers (JEOL J7600F, JEOL

JSM-6010/LA). All metallographic preparations were done in dry conditions in order to avoid dissolution of hygroscopic Cl-containing compounds. Corrosion product scales (oxide, sulfide…) were removed from specimens used to evaluate the weight loss by chemical washing following ISO/DIS 17248 standard [22]. Inconel 625 samples were dipped in a heated (60 °C) solution containing 18% of sodium hydroxide and 3% of potassium permanganate during 20-30 minutes, then in a solution of ammonium citrate (10%) in the same conditions. 16Mo3 samples were dipped in hydrochloric acid (20%) doped with hexamethylene tetramine. The washed samples were weighed and the masses were compared to those before test. Preliminary tests have shown that none of the two alloys were corroded in chemical washing solutions.

Results and discussion

In the first part of this paper, preliminary tests that led to choose the heavy metal chloride ash composition are presented. Then, chemistry of synthetic ashes containing zinc chloride is discussed. Afterward, the discussion in the two next parts will be focused on the mass losses and then the thickness losses of both materials versus time in # $ZnCl_2$ ash at 450 °C and compared to results obtained a higher temperature in zinc chloride free ashes (# 10% Cl and # 40% Cl ashes). Finally, the SEM/EDX studies of the corrosion products formed on tested materials are presented and discussed and also compared to corrosion profiles observed in ashes without $ZnCl_2$.

Preliminary tests

In order to study the influence of the presence of heavy metal chlorides on corrosion kinetics, three ash compositions have been considered based on # 10% Cl containing alkali chloride ash with an addition of 10 wt% of heavy metal chloride (Table 2). The content of NaCl, KCl, Na_2SO_4 and K_2SO_4 is constant and the balance is done with $CaSO_4$. Preliminary tests have been performed to give a first estimation of the corrosivity of those synthetic ashes by measuring mass losses on 16Mo3 and Inconel

625 alloys after 100 h of exposure at 650 °C. Results of those tests are presented on Fig. 2. Mass losses are close in # 40% Cl and # 10% Cl ashes after 100 h of exposure. The three ashes containing heavy metal chlorides have led to high mass losses (up to 6 times bigger than those measured in heavy metal free ashes) which reached 315 mg/cm^2 for 16Mo3 steel in # $ZnCl_2$/$PbCl_2$ ash and 100 mg/cm^2 for Inconel 625 alloy in # $ZnCl_2$ ash. Mass losses measured in # $PbCl_2$ were the lowest of the three heavy metal chlorides ashes. Mass losses in the two other ashes (# $ZnCl_2$ and # $ZnCl_2$/$PbCl_2$) are in the same range. The # $ZnCl_2$ ash has been finally chosen for the rest of the study because the melting point of zinc chloride is the lowest one (320 °C, [23]), and as it was also the most corrosive ash (especially for Inconel 625). Furthermore, this choice allowed the addition of only one other specie to the 5 components salt mixture.

Chemistry of ashes

It has been shown [11] that corrosion rates were correlated with the presence and proportion of molten phases and so, with the solidus temperature. Furthermore, heavy metal chlorides have low melting point and their presence in ash is known to decrease temperature of melt and thus, increase corrosion rate at lower temperature [9,24]. Two complementary methods (DTA and TMA) have been combined to measure the solidus temperature of # $ZnCl_2$ ash. Obtained results are reported in Table 3 and compared to those measured previously on # 10% Cl and # 40% Cl. Both measurement methods were in good agreement and showed that the presence of $ZnCl_2$ in ash mixture decreased drastically T_{sol} from 510 °C to 355 °C. It has been shown in our last study that $CaSO_4$ can be considered as spectator specie in the mixture and only play an effective role on the melt fraction. This melt fraction represents 20 wt% in # 10% Cl ash and 50 wt% in # 40% Cl at 650 °C. From the conclusion on zinc free chloride ashes, the maximum liquid fraction reached at 650 °C corresponds to the sum fraction of all species without $CaSO_4$ [11]. Thus, it can be considered that the fraction of melt in this mixture is 30 wt%. This is confirmed by macroscopic observations on samples: only a small part of the ash mixture is melted.

Presence of molten phases at 450 °C in # $ZnCl_2$ ash is supposed to induce higher corrosion compared to salts (# 10% Cl and # 40% Cl) without molten phases at the same temperature.

Corrosion tests

Mass lossFig. 3 and 4 show mass losses of 16Mo3 and Inconel 625 at 450 °C in # $ZnCl_2$ ash and at 650 °C in # 10% Cl and # 40% Cl ashes as a function of time. Mass losses of both alloys at 650 °C in zinc chlorides ash after 100 h are also represented on the graph (Fig. 3 and 4). They correspond to the preliminary tests discussed previously. Mass losses measurements gave an average metal loss but did not take into account localized corrosion instead of thickness loss measurements. It has to be considered that the straight lines connecting the dots are not relevant and have been added to help readers. Molten fraction of each ash mixture is also indicated on the graph. In all tested conditions, Inconel 625 samples were less corroded than 16Mo3. Mass losses observed on samples exposed to # $ZnCl_2$ ash at 450 °C were much more important than those observed for ashes without $ZnCl_2$ at 650 °C. As it has been shown [11], low mass losses were observed at 450 °C in salts without $ZnCl_2$ (less than 10 mg/cm^2 for 16Mo3 after 1000 h in both # 10% Cl and # 40% Cl ashes and close to 0 for Inconel 625), due to the absence of molten phases at this low temperature. In # $ZnCl_2$ ash, the highest mass loss was observed on 16Mo3 (A, about 320 mg/cm^2). In the same ash, the highest mass loss of Inconel 625 was observed after 1000 h of exposure (E, about 225 mg/cm^2). At 650 °C in ashes without $ZnCl_2$, the highest mass losses were observed after 1000 h of exposure in # 40% Cl ash for both 16Mo3 (C, about 160 mg/cm^2) and Inconel 625 (G, about 90 mg/cm^2). So, the addition of only 10 wt% of $ZnCl_2$ in the ash led to multiplicate the corrosion rate by five after 1000 h for the nickel based alloy, and by two for the 16Mo3 steel. In addition, mass loss of 16Mo3 after 100 h at 650 °C in # $ZnCl_2$ ash was about 280 mg/cm^2 (D) and close to 100 mg/cm^2 for Inconel 625 (H). Those values, observed after 100 h (D and H), were up to twice higher than those observed in # 10% Cl ash (without $ZnCl_2$) after 1000 h of exposure at 650 °C for 16Mo3 and up to three times higher for Inconel 625 (B and F). This plot already exhibits the high corrosivity of $ZnCl_2$ even at low temperature due to the presence of

molten phases at low temperature as demonstrated in chemistry of salt mixture section. It should also be noted that higher corrosion was observed in # $ZnCl_2$ ash than in # 40% Cl even if the last one have a higher molten fraction. Few studies are presenting mass loss of samples in representative ashes with heavy metal chlorides and none in similar conditions to the present ones. Nevertheless, the high corrosivity of heavy metal chloride has already been studied [25] by measuring corrosion products thickness. Thicknesses of those corrosion products were much higher in presence of heavy metal chlorides in deposit.

Thickness loss

Fig. 5 and 6 show the thickness losses of 16Mo3 and Inconel 625 after exposure to # $ZnCl_2$ ash at 450 °C versus time compared to # 10% Cl (Fig. 5) and # 40% Cl (Fig. 6) ashes at 650 °C. The maximum thickness loss observed for 16Mo3 alloy was about 615 µm in # $ZnCl_2$ ash after 1000 h at 450 °C while for Inconel 625 alloy, the maximum was about 410 µm in the same conditions of corrosion. Those results were in good agreement with mass losses discussed in the previous part. As observed by mass loss measurements, those of thickness loss in # $ZnCl_2$ were twice higher than those observed on both alloys in salts without $ZnCl_2$ (and up to four times higher than for 16Mo3 exposed to ash with and without $ZnCl_2$ after 1000 h of exposure). Contrary to mass loss, thickness loss gave more information on local corrosion. Indeed, the thickness loss was an average of twenty measurements and the error bar gave also a minimum and a maximum of thickness loss which reflected localized corrosion. The standard deviations obtained for samples exposed to # $ZnCl_2$ ash were up to four times bigger than those in ash without $ZnCl_2$ and underlined a less homogenous attack.

SEM/EDX studies of the corrosion products in zinc chloride ash

Fig. 7 presents the SEM global view of 16Mo3 (a,b) and Inconel 625 (c,d) samples after 500 h at 650 °C in # 10% Cl ash (a,c) and at 450 °C in # $ZnCl_2$ ash (b,d). A stronger attack was observable and

a high internal attack by pitting at grains boundaries was perceptible in # $ZnCl_2$ ash, especially for the iron-based alloy. Inconel 625 sample exposed to # $ZnCl_2$ ash also exhibited a non-uniform attack. The corrosion profiles for each sample are described below.

16Mo3

Fig. 8 shows SEM images of 16Mo3 sample after 500h of exposure to # $ZnCl_2$ ash at 450 °C. Even if the test was performed at low temperature, severe corrosion was observed. The corrosion profile was very different of the one observed at the same temperature without $ZnCl_2$ (described in [11]) and looked like a high temperature corrosion profile. Oxide layers were mixed with ashes compounds and strong internal attack by chlorine (pitting corrosion) was observed and seemed to propagate along the grain boundaries as shown on Fig. 9. Measured pits were about 80 µm deep. Reaction between chlorides and oxide seemed to be occurring here since salt elements (Ca, K, S) were detected into oxide layer as shown on X element maps (Fig. 8). Small amounts of zinc salt were detected in the entire oxide layer and not systematically associated with chlorine. The thickness of those oxide scales was up to 2000 µm, and mainly composed of iron oxide, zinc and iron mixed oxide and a few iron sulphur (according to EDS analysis).

Inconel 625

Fig. 10 shows SEM images of Inconel 625 sample after 500 h of exposure to # $ZnCl_2$ ash at 450 °C. It was also severely attacked at this low temperature. Thickness of corrosion products was about 500 µm. Internal pitting was also detected with a depth about 20 µm. Chromium oxide was the main corrosion product observed above metal/oxide interface but it is porous and mixed with salt mixture compounds (chloride and sulfates). The upper part of the oxide scale was composed of mixed oxides (Cr, Zn, Mo), chlorides and sulfates enriched in Ni. Zinc salt was detected in the entire oxide layer and not only associated with chlorine. Contrary to profiles observed at 650 °C without $ZnCl_2$ (also described in [11]), no chromium free zone was observed at metal/oxide interface and no separate corrosion products scales (Cr_2O_3, NiS, NiO) were present.

Discussion

In presence of $ZnCl_2$ in the salt mixtures, the corrosion profile observed for 16Mo3 samples at 450 °C is quite the same as the one observed at higher temperature (650 °C) without $ZnCl_2$. However, the corrosion was more severe and exhibited an extremely high internal attack. Presence of $ZnCl_2$ in the molten phase containing also alkali chlorine and sulfate is assumed to be responsible of such attack since its presence is the only difference between the ashes (particularly between # $ZnCl_2$ and # 10% Cl ash). The attack was assumed to be due to fluxing of the protective oxide following reactions proposed by BANKIEWICZ [25] and illustrated in Fig. 13 in addition of reactions described without $ZnCl_2$ in deposit [11]:

$ZnCl_2$ (l) + Fe_3O_4 = $ZnFe_2O_4$ + $FeCl_2$ (g) $\Delta G°$ (450 °C) = 19 kcal/mol [26] (1)

3 $ZnCl_2$ (l) + 2 Fe_3O_4 + O_2 (g) = 3 $ZnFe_2O_4$ + 3 Cl_2 (g) $\Delta G°$ (450 °C) = -12 kcal/mol [26] (2)

Gibbs free energies of each reaction versus temperature are presented in Fig. 12. $ZnCl_2$ can also react directly with iron:

$ZnCl_2$ (l) + Fe + 2 O_2 (g) = $ZnFe_2O_4$ + Cl_2 (g) $\Delta G°$ (450 °C) = -148 kcal/mol [26] (3)

$ZnCl_2$ can also contribute to form Cl_2 (g) by direct oxidation even if this reaction is less favored from thermodynamic point of view:

$ZnCl_2$ (l) + ½ O_2 (g) = ZnO + Cl_2 (diss) $\Delta G°$ (450 °C) = 8 kcal/mol [26] (4)

The chlorine formed by reactions 1-4 can attack the iron at interface as described in [11]:

Fe + Cl_2 (g) = $FeCl_2$ (s,g) $\Delta G°$ (450 °C) = -43 kcal/mol [26] (5)

Contrary to 16Mo3 samples, corrosion profile observed on Inconel 625 samples in presence of $ZnCl_2$ is very different from those observed at higher temperature (650 °C) in absence of $ZnCl_2$ in ash. The attack is also severe (as for 16Mo3) but no stratification was observed contrary to profiles presented in

[11] after exposure to # 10% Cl and # 40% Cl at 650 °C. All corrosion products are mixed, which is a clear sign of fluxing mechanism probably coupled with direct attack of metal by molten chloride. Formation of initial Cr_2O_3 layer is also probable considering the high Cr content in Inconel 625 (23%.wt) and the oxidizing condition assumed as the tests are performed in laboratory air. Nevertheless it is obvious that formed Cr_2O_3 was no longer protective (non continuous, non adhesive). The role of $ZnCl_2$ contained in the molten salts can be described by the following reactions:

$ZnCl_2$ (l) + 2 Cr + 2 O_2 (g) = $ZnCr_2O_4$ + Cl_2 (g) $\Delta G°$ (450 °C) = -232 kcal/mol [26] (6)

2 $ZnCl_2$ (l) + 2 Cr_2O_3 + O_2 (g) = 2 $ZnCr_2O_4$ + 2 Cl_2 (g) $\Delta G°$ (450 °C) = -14 kcal/mol [26] (7)

ZnO from reaction 4 can also dissolve chromium oxide:

ZnO + Cr_2O_3 = $ZnCr_2O_4$ $\Delta G°$ (450 °C) = -15 kcal/mol [26] (8)

The stages of the corrosion of the Inconel 625 in synthetic # $ZnCl_2$ ash are schematically represented in Fig. 11. The strong internal attack by pitting at grains boundaries observed on both 16Mo3 and Inconel 625 was assumed to be favored by the presence of a low viscosity (high wettability) molten phase due to $ZnCl_2$ addition. By comparing thickness and mass losses in ashes with and without $ZnCl_2$ and molten fraction of each ash, it also appeared that the chloride specie was more important than the molten fraction. Indeed, thickness and mass losses observed were much more important in # $ZnCl_2$ ash with a molten fraction of 0.3 than in # 40% Cl ash which had a molten fraction of 0.5.

Conclusion

The purpose of this study was to evaluate the influence of zinc chloride content in synthetic ashes representative of Waste-to-Energy deposits on the relative resistance of two heat exchanger materials. After preliminary tests, a synthetic ash containing 10 wt% of $ZnCl_2$ has been chosen to evaluate the corrosion of metallic alloys (16Mo3 and Inconel 625). Corrosion tests were performed in air at 450 °C and compared to those run at 650 °C [11] (without $ZnCl_2$). Temperatures of solidus of ashes have been determined using two different methods: DTA, TMA.

■ The measured temperature indicated that molten phases were already present at 450 °C ($T_{solidus}$ = 320°C), which is the temperature of corrosion tests, but is also representative of current metal tube operating conditions.

■ In presence of $ZnCl_2$ in ash, both alloys exhibited high corrosion rate at 450 °C compared to very low attack without $ZnCl_2$ at the same temperature. Corrosion observed with $ZnCl_2$ at 450 °C was twice more important than without $ZnCl_2$ at 650 °C.

■ $ZnCl_2$ induced presence of highly corrosive molten phases at this temperature, and fluxing mechanisms occurred.

■ The strong internal attack by pitting (intergranular attack) at grains boundaries observed on both 16Mo3 and Inconel 625 was assumed to be due to a low viscosity molten phase induced by $ZnCl_2$. Lower viscosity of the molten phase in presence of $ZnCl_2$ should led to higher wettability of the molten phases within oxide scale cracks and pores. Viscosity measurements should confirm this hypothesis.

■ Furthermore, it seems that the chloride specie is more important than the molten fraction since corrosion observed in # 40% Cl ash with a molten fraction of 0.5 was lower than in # $ZnCl_2$ ash which has a molten fraction of 0.3.

■ Both evaluation methods, thickness loss and mass loss, were in good agreement and showed that presence of zinc chloride in ash led to high corrosion rate at low temperature and non uniform attack, due to the presence of molten phases and the highly corrosive character of $ZnCl_2$ compared to alkali chlorides.

Acknowledgements This work has been supported by the French National Research Agency with project ANR SCAPAC 11-RMNP-0016 in partnership with, AIR LIQUIDE, SEDIS and CIRIMAT/ENSIACET. The authors thank L. ARANDA of Institut Jean Lamour, Nancy (France) for carrying out TMA and DTA analyses.

Table 1 Elemental metallic alloy compositions (wt%)

	Composition (wt%)											
	Ni	Fe	Cr	Mo	Nb	Mn	Si	C	Cu	Co	Ti	Al
16Mo3	-	Bal.	0.3	0.3	-	0.9	0.35	0.2	0.3	-	-	-
Inconel 625	Bal.	4	22	9	3.5	0.5	0.35	0.08	0.3	1.0	0.9	0.5

Table 2 Composition (wt%) of the synthetic ashes

	Composition (wt%)						
	NaCl	KCl	Na_2SO_4	K_2SO_4	$CaSO_4$	$ZnCl_2$	$PbCl_2$
# 40% Cl	20	20	5	5	50	-	-
# 10% Cl	5	5	5	5	80	-	-
# $ZnCl_2$	5	5	5	5	70	10	-
# $PbCl_2$	5	5	5	5	70	-	10
# $ZnCl_2/PbCl_2$	5	5	5	5	70	5	5

Table 3 Solidus and liquidus temperatures of ashes measured with DTA and TMA

Composition (wt%)	DTA (°C)	TMA (°C)

Ashes	NaCl	KCl	Na_2SO_4	K_2SO_4	$CaSO_4$	$ZnCl_2$	T_{sol}	T_{liq}	T_{sol}	T_{liq}
# 10% Cl without $CaSO_4$	25	25	25	25	-	-	512	560	525	-
# 10% Cl	5	5	5	5	80	-	510	550	-	-
# 40% Cl without $CaSO_4$	40	40	10	10	-	-	511	615	548	-
# 40% Cl	20	20	5	5	50	-	508	595	520	-
# $ZnCl_2$ without $CaSO_4$	16.7	16.7	16.7	16.7	-	33.3	348	-	315	-
# $ZnCl_2$	5	5	5	5	70	10	355	-	329	-

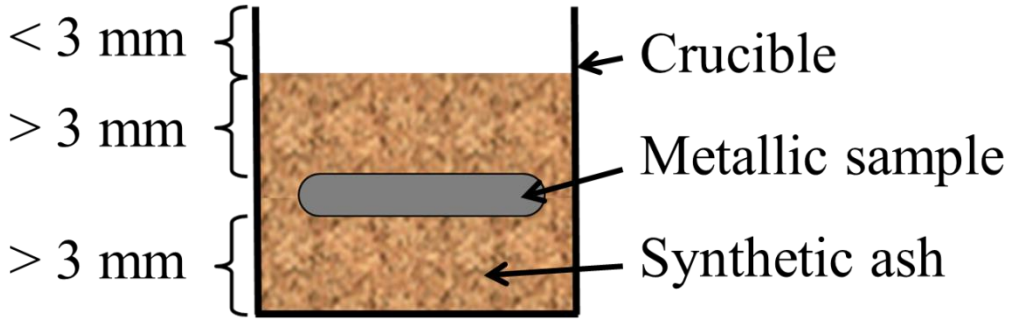

Fig. 1 Scheme of corrosion test settings

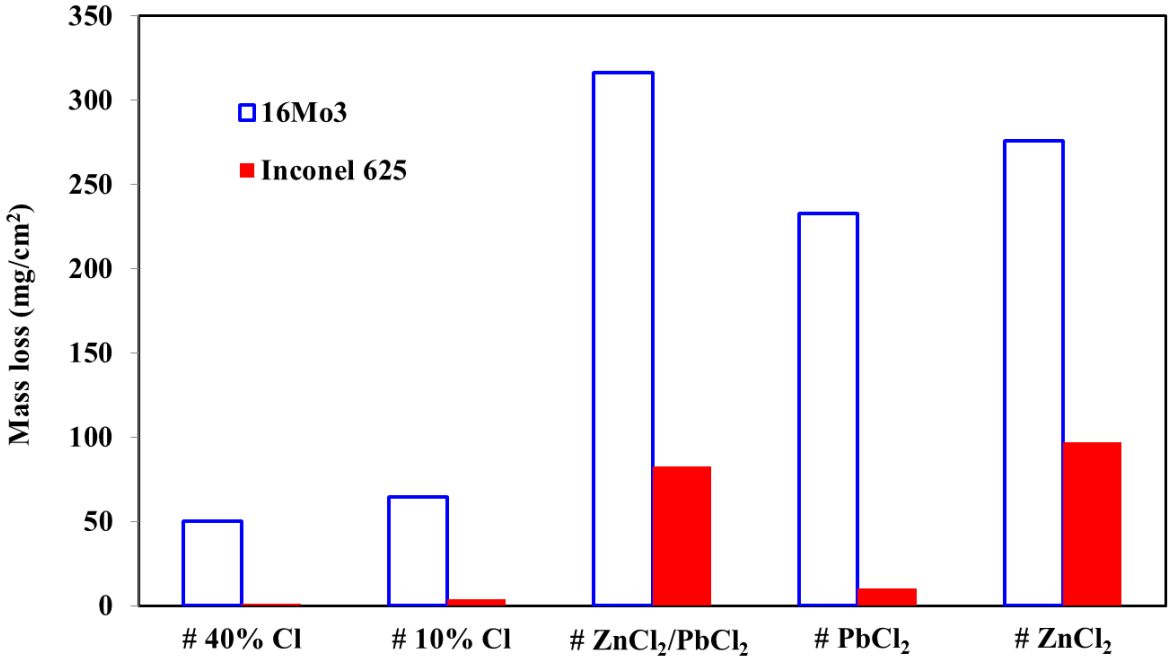

Fig. 2 Mass loss measured on 16Mo3 steel and on Inconel 625 alloy after 100 h of exposure at 650 °C to # 10% Cl and # 40% Cl ashes, and at 450 °C to # $ZnCl_2/PbCl_2$, # $PbCl_2$ and # $ZnCl_2$ ashes

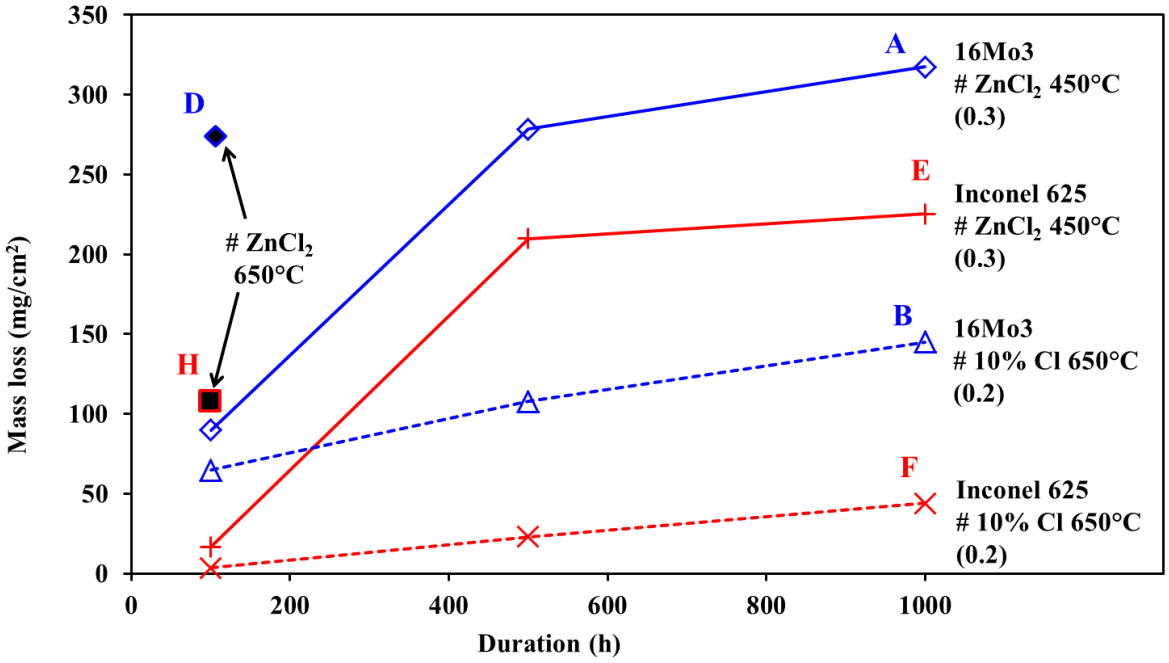

Fig. 3 Mass loss measured on 16Mo3 steel and on Inconel 625 alloy after exposure to # 10% Cl and # $ZnCl_2$ ashes versus time (h). The estimated molten phase fraction in ash mixture is indicated by (X.X). Doted and straight lines are guide for the eyes in order to emphasize the two kinetics below and above T_{sol}

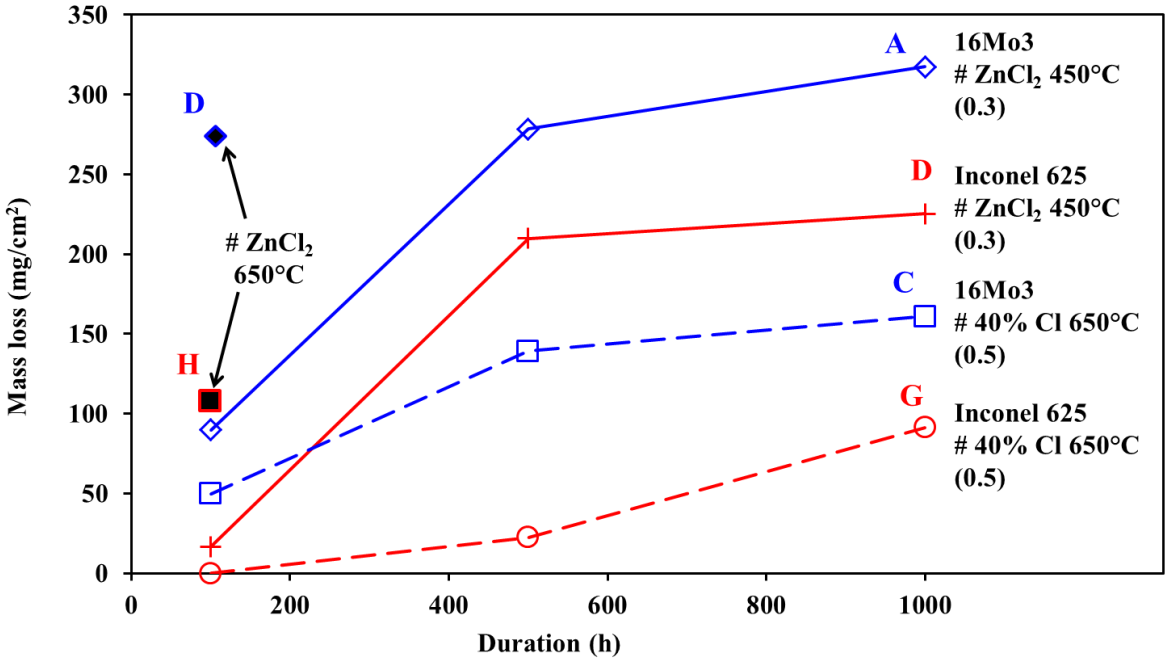

Fig. 4 Mass loss measured on 16Mo3 steel and on Inconel 625 alloy after exposure to # 40% Cl and # $ZnCl_2$ ashes versus time (h). The estimated molten phase fraction in ash mixture is indicated by (X.X).

Doted and straight lines are guide for the eyes in order to emphasize the two kinetics below and above T_{sol}

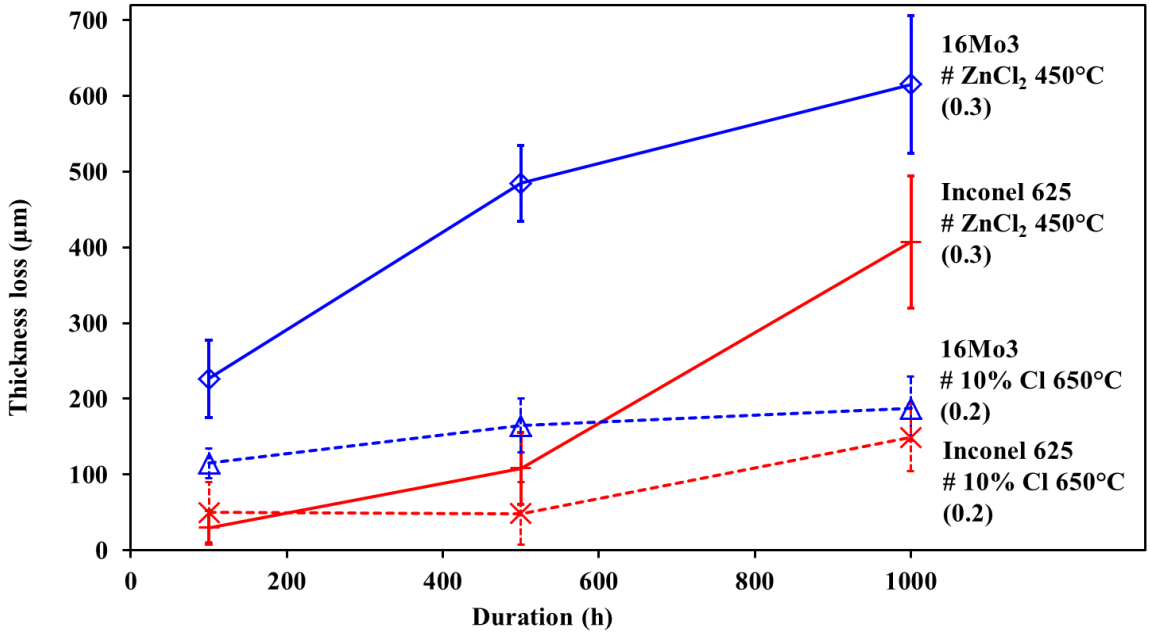

Fig. 5 Thickness loss measured on 16Mo3 steel and Inconel 625 alloy after exposure to # 10% Cl and # $ZnCl_2$ ashes versus time (h). The estimated molten phase fraction in ash mixture is indicated by (X.X). Doted and straight lines are guide for the eyes in order to emphasize the two kinetics below and above T_{sol}

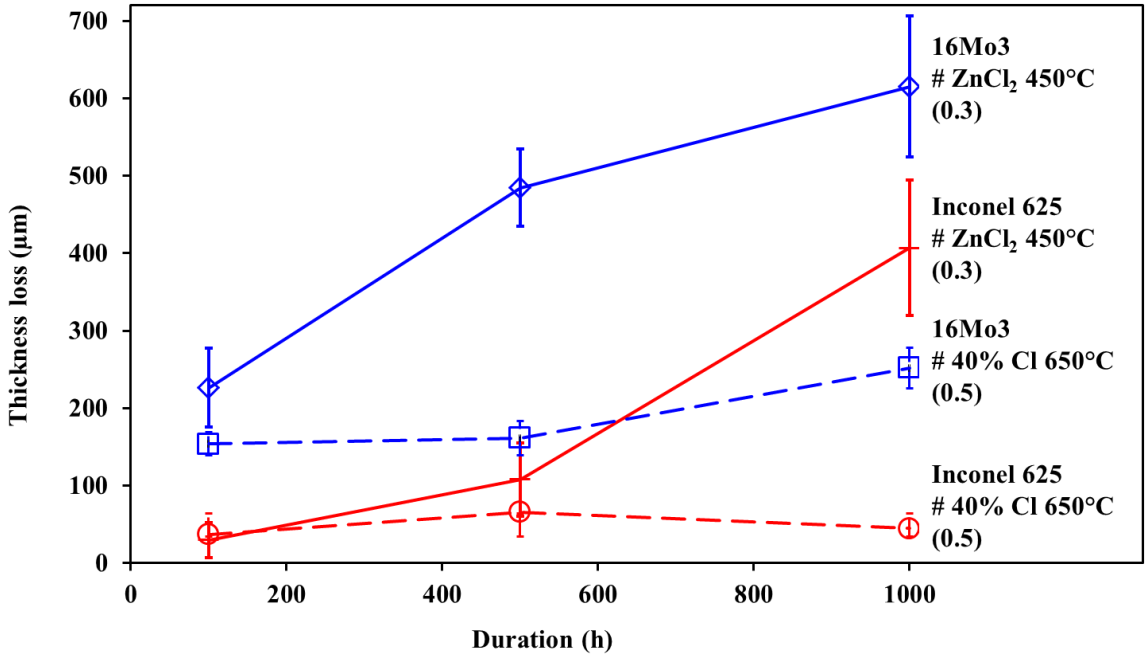

Fig. 6 Thickness loss measured on 16Mo3 steel and Inconel 625 alloy after exposure to # 40% Cl and # $ZnCl_2$ ashes versus time (h). The estimated molten phase fraction in ash mixture is indicated by (X.X). Doted and straight lines are guide for the eyes in order to emphasize the two kinetics below and above T_{sol}

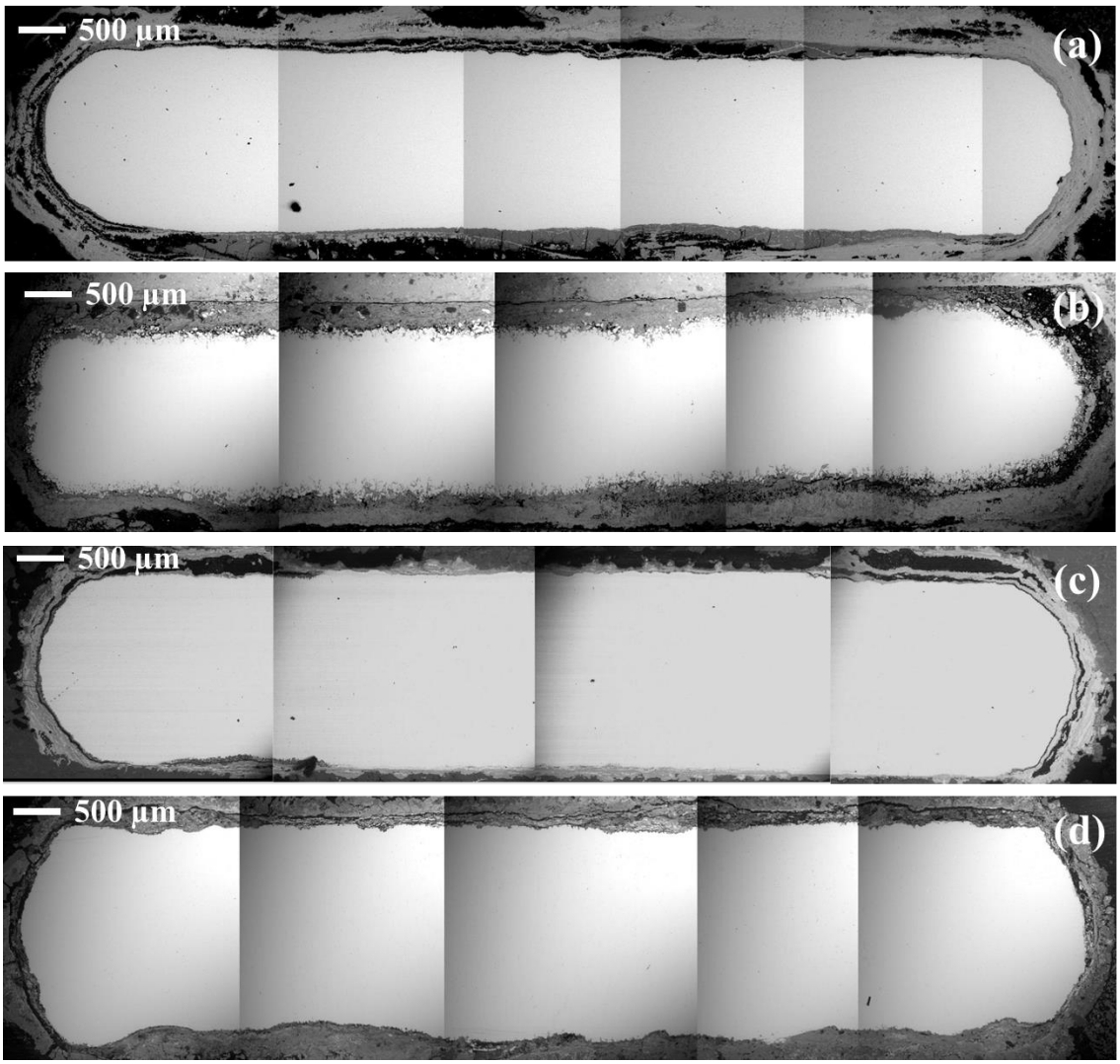

Fig. 7 SEM pictures of 16Mo3 steel (a,b) and Inconel 625 alloy (c,d) after 500 h at 650 °C in # 10% Cl ash (a,c) and at 450 °C in # $ZnCl_2$ ash (b,d)

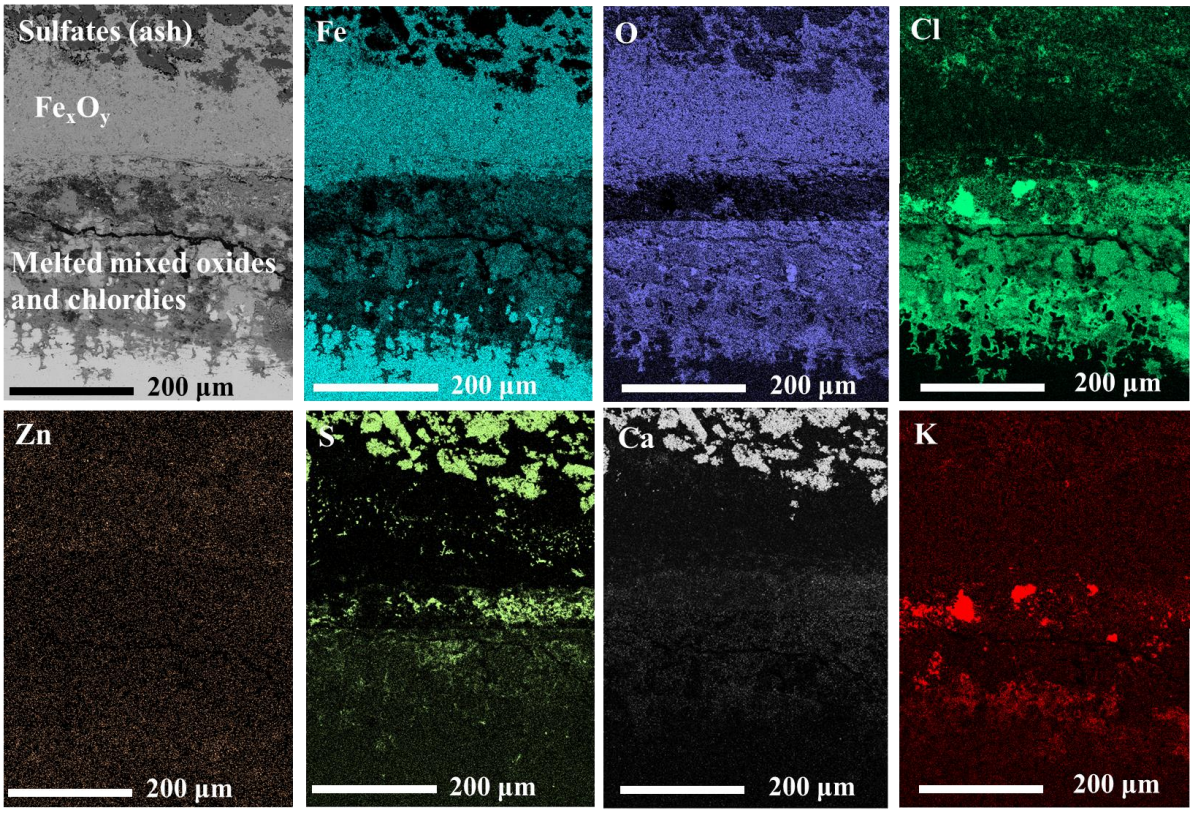

Fig. 8 Cross section of 16Mo3 steel after 500 h exposure in # $ZnCl_2$ ash (a) at 450 °C and X element maps (b)

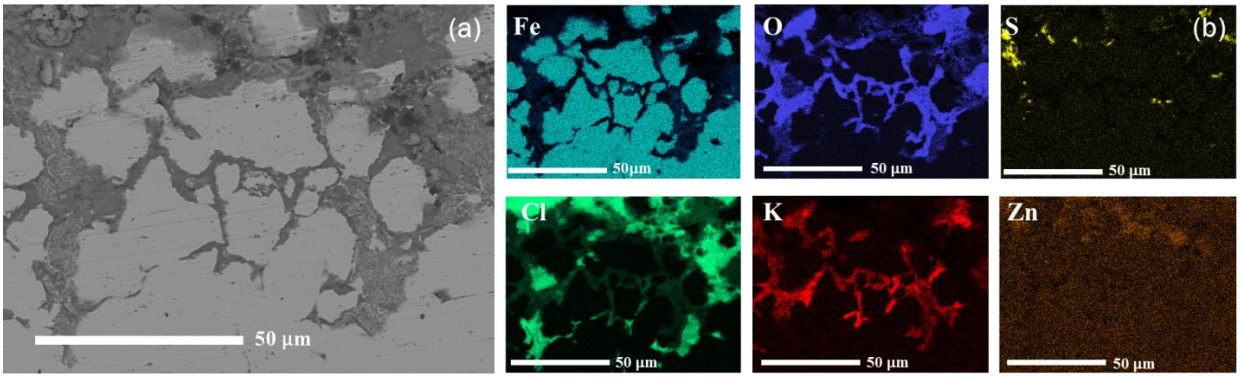

Fig. 9 Zoom on internal pitting of 16Mo3 steel after 500 h exposure in # $ZnCl_2$ ash (a) at 450 °C and X element maps (b)

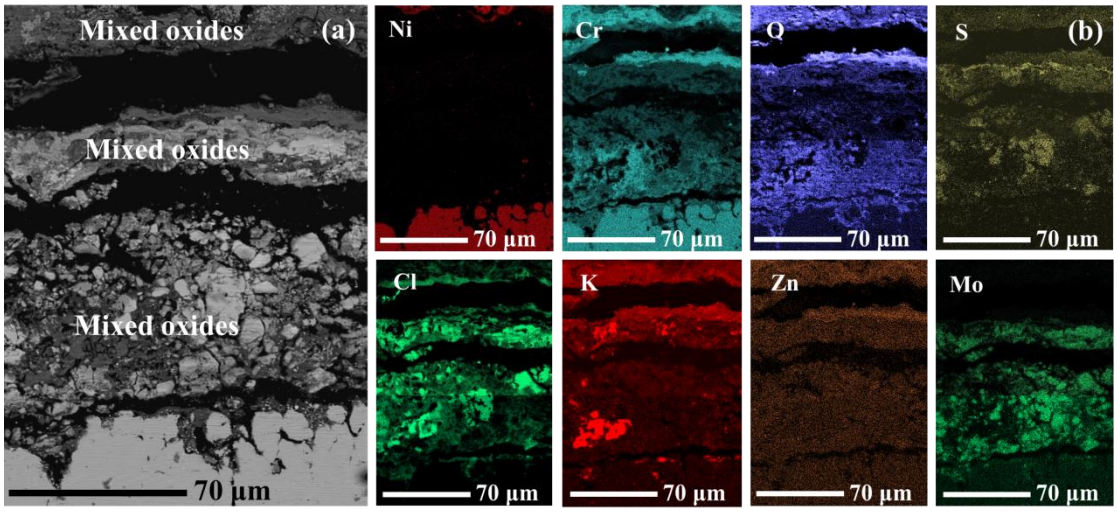

Fig. 10 Cross section of Inconel 625 steel after 500 h exposure in # $ZnCl_2$ ash (a) at 450 °C and X element maps (b)

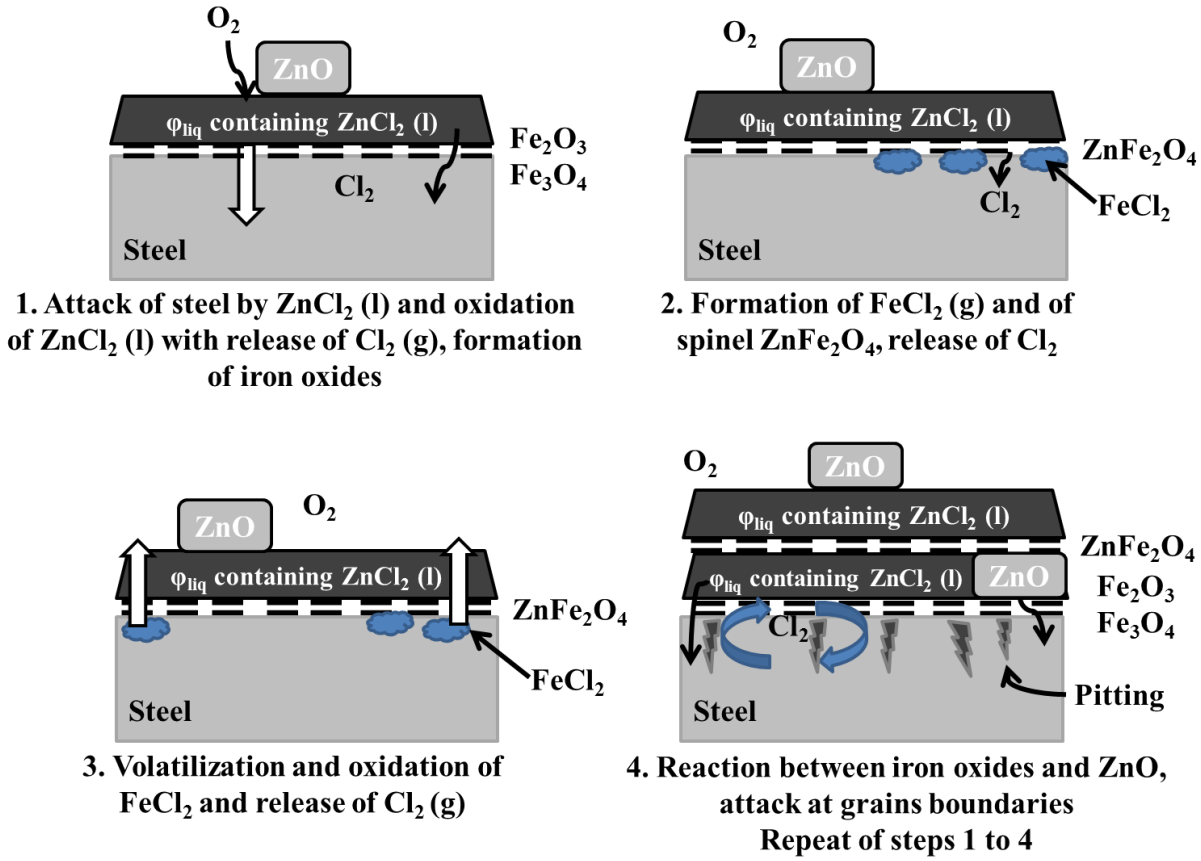

Fig. 11 Corrosion mechanism of Fe-based alloy by $ZnCl_2$ containing ash (φ_{liq} = liquid phase)

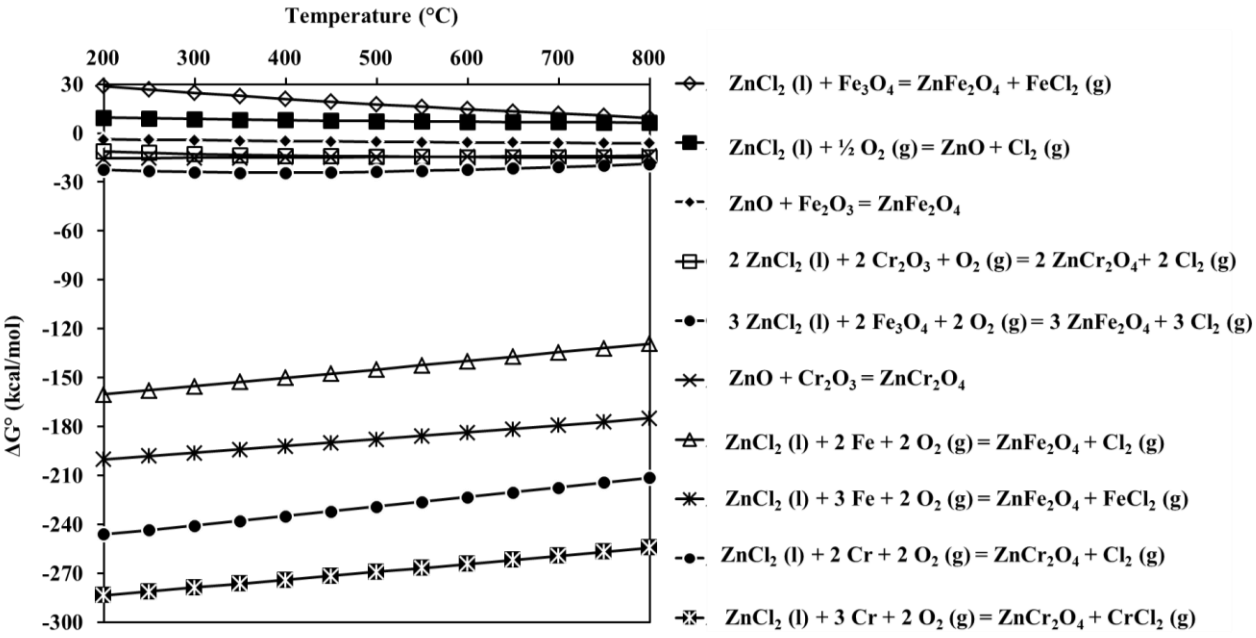

Fig. 12 Gibbs free energy of iron and chromium reactions as a function of temperature (°C)

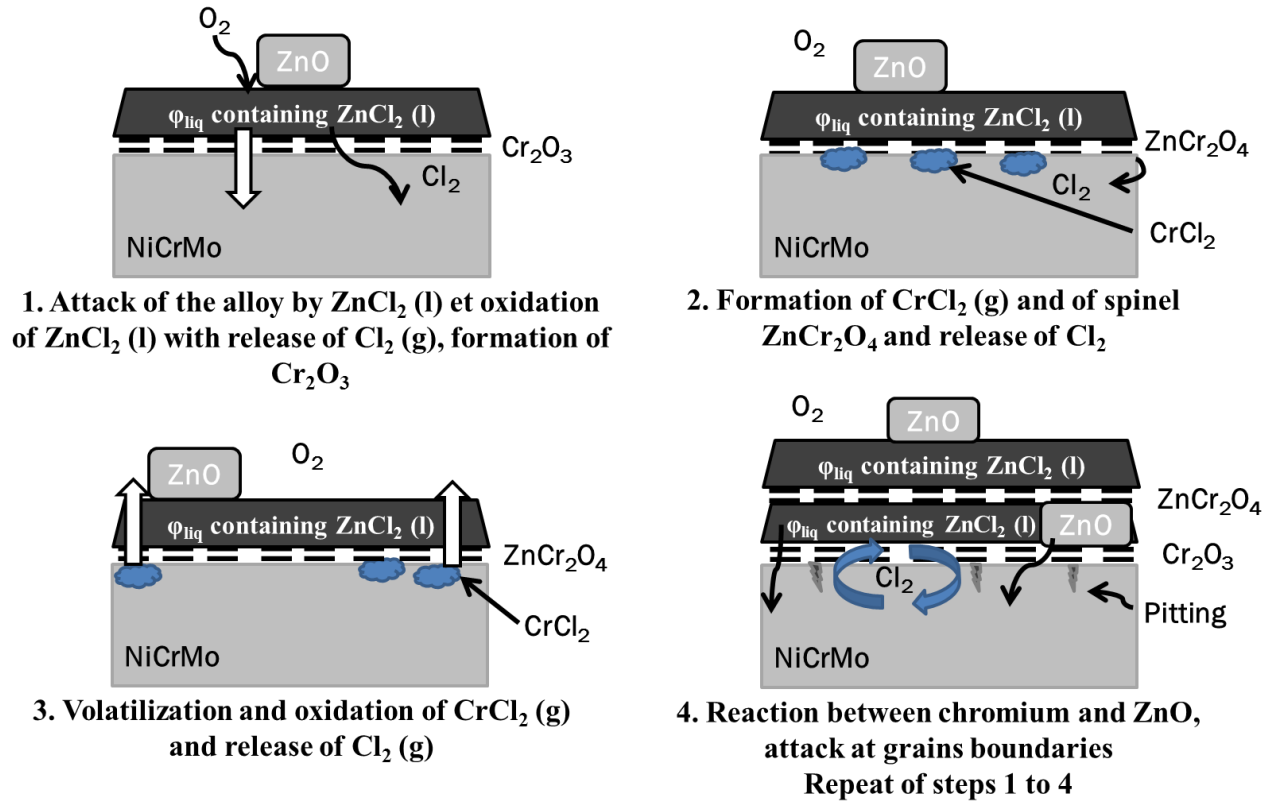

Fig. 13 Corrosion mechanism of Ni-based alloy by $ZnCl_2$ containing ash (φ_{liq} = liquid phase)

References

[1] Kawahara, Y. (2002). High temperature corrosion mechanisms and effect of alloying elements for materials used in waste incineration environment. Corrosion science, 44(2), 223-245.

[2] Pedersen, A. J., Frandsen, F. J., Riber, C., Astrup, T., Thomsen, S. N., Lundtorp, K., Mortensen, L. F. (2009). A Full-scale Study on the Partitioning of Trace Elements in Municipal Solid Waste Incineration · Effects of Firing Different Waste Types†. Energy & Fuels, 23(7), 3475-3489.

[3] Becidan, M., Sørum, L., Frandsen, F., Pedersen, A. J. (2009). Corrosion in waste-fired boilers: a thermodynamic study. Fuel, 88(4), 595-604.

[4] Talonen, T. (2008). Chemical equilibria of heavy metals in waste incineration: comparison of thermodynamic databases. Lic. Thesis. Åbo Akademi University, Finland.

[5] Zhang, Y. L., Kasai, E. (2004). Effect of chlorine on the vaporization behavior of zinc and lead during high temperature treatment of dust and fly ash. ISIJ international, 44(9), 1457-1468.

[6] Bøjer, M., Jensen, P. A., Frandsen, F., Dam-Johansen, K., Madsen, O. H., Lundtorp, K. (2008). Alkali/Chloride release during refuse incineration on a grate: Full-scale experimental findings. Fuel Processing Technology, 89(5), 528-539.

[7] Osada, S., Kuchar, D., Matsuda, H. (2009). Effect of chlorine on volatilization of Na, K, Pb, and Zn compounds from municipal solid waste during gasification and melting in a shaft-type furnace. Journal of Material Cycles and Waste Management, 11(4), 367-375.

[8] Chan, C., Jia, C. Q., Graydon, J. W., & Kirk, D. W. (1996). The behaviour of selected heavy metals in MSW incineration electrostatic precipitator ash during roasting with chlorination agents. Journal of Hazardous Materials, 50(1), 1-13.

[9] Spiegel, M. (1999). Salt melt induced corrosion of metallic materials in waste incineration plants. Materials and Corrosion, 50(7), 373-393.

[10] Li, Y. S., Niu, Y., Wu, W. T. (2003). Accelerated corrosion of pure Fe, Ni, Cr and several Fe-based alloys induced by ZnCl 2–KCl at 450 C in oxidizing environment. Materials Science and Engineering: A, 345(1), 64-71.

[11] Schaal, E., David, N., Panteix, P. J., Rapin, C., Brossard, J. M., Maad, F. (2015). Effect of Chloride Content in Ash in Oxidation Kinetics of Ni-Based and Fe-Based Alloys. Oxidation of Metals, 84 (3), 307-327.

[12] Lehmusto, J., Yrjas, P., Skrifvars, B. J., Hupa, M. (2012). High temperature corrosion of superheater steels by KCl and K 2 CO 3 under dry and wet conditions. Fuel Processing Technology, 104, 253-264.

[13] Pettersson, J., Folkeson, N., Johansson, L. G., Svensson, J. E. (2011). The effects of KCl, K2SO4 and K2CO3 on the high temperature corrosion of a 304-type austenitic stainless steel. Oxidation of metals, 76(1-2), 93-109.

[14] Bankiewicz, D., Yrjas, P., Lindberg, D., Hupa, M. (2013). Determination of the corrosivity of Pb-containing salt mixtures. Corrosion Science, 66, 225-232.

[15] Jonsson, T., Folkeson, N., Svensson, J. E., Johansson, L. G., Halvarsson, M. (2011). An ESEM in situ investigation of initial stages of the KCl induced high temperature corrosion of a Fe–2.25 Cr–1Mo steel at 400 C. Corrosion Science, 53(6), 2233-2246.

[16] Varis, Bankiewicz, T. D., Yrjas, P., Oksa, M., Suhonen, T., Tuurna, S., Ruusuvuori, K., Holmström, S. (2015) High temperature corrosion of thermally sprayed NiCr and FeCr coatings covered with a KCl–K2SO4 salt mixture. Surface & Coatings Technology 265, 235-243.

[17] Ruh, A., Spiegel, M. (2006). Thermodynamic and kinetic consideration on the corrosion of Fe, Ni and Cr beneath a molten KCl–ZnCl 2 mixture. Corrosion science, 48(3), 679-695.

[18] Li, Y. S., Spiegel, M., Shimada, S. (2005). Corrosion behaviour of various model alloys with NaCl–KCl coating. Materials Chemistry and Physics, 93(1), 217-223.

[19] Lehmusto, J., Skrifvars, B. J., Yrjas, P., Hupa, M. (2011). High temperature oxidation of metallic chromium exposed to eight different metal chlorides. Corrosion Science, 53(10), 3315-3323.

[20] Enestam, S., Bankiewicz, D., Tuiremo, J., Mäkelä, K., Hupa, M. (2013). Are NaCl and KCl equally corrosive on superheater materials of steam boilers?. Fuel, 104, 294-306.

[21] Bale, C. W., Chartrand, P., Degterov, S. A., Eriksson, G., Hack, K., Mahfoud, R. B. Melancon, J., Pelton, A. A., Petersen, S. (2002). FactSage thermochemical software and databases. Calphad, 26(2), 189-228.

[22] ISO/DIS 17248, *AFNOR*, (2014)

[23] Lushnaya, N. P., Evseeva, N. N., Vereshchetina, I. P. (1956). Physical properties of salt melts and the nature of their structural parts. Russian Journal of Inorganic Chemistry, 1(7), 35-45.

[24] Sánchez Pastén, M., Spiegel, M. (2006). High temperature corrosion of metallic materials in simulated waste incineration environments at 300–600 C. Materials and Corrosion, 57(2), 192-195.

[25] Bankiewicz, D., Enestam, S., Yrjas, P., Hupa, M. (2013). Experimental studies of Zn and Pb induced high temperature corrosion of two commercial boiler steels. Fuel Processing Technology, 105, 89-97.

[26] Roine, A. (1999). HSC Chemistry Version 4.1. Outokumpu Research Organization, Pori, Finland.